Mechanical Performance of Geopolymer Mortar Incorporating Fly Ash Based Sand as an Alternate Construction Material

Kummari Sekhar[1]; Vesna Zalar Serjun[2]; and Bendadi Hanumantha Rao[3]

Abstract: The construction industry for a long time looking a substitute for fine aggregates (i.e., sand) because of ever depleting river sand deposits and implementing stringent sand mining regulations. Development of such alternate fine aggregate using an affluently available industrial by-product is commendable. This study endeavors to develop geopolymer mortar (GPM) using fly ash based sand (FAB sand) as an alternate fine aggregate, demonstrates its performance by comparing with river sand and proposes a suitable mix design methodology for the same. The novelty of the study lies in replacing river sand (100%) with FAB sand to manufacture GPM and thus, propose FAB sand as a potential novel construction material. Two sets of GPM cubes, one with 100% FAB sand while the other with 100% river sand, are made, considering NaOH molarity of 10, $Na_2SiO_3/NaOH$ ratio of 1.5, curing temperature of 60 & 80°C, and curing period of 7, 14, and 28 days. Flowability, compressive strength, water absorption, morphological, and mineralogical properties of GPM cubes are further assessed. The results evidently show a high compressive strength of GPM cubes made with FAB sand. The findings of the study elucidate that FAB sand is a doable and practicable alternative to river sand in construction applications. **DOI: 10.1061/JMCEE7.MTENG-21941.**

Author keywords: Fly ash; Fly ash based (FAB) sand; River sand; Alternate fine aggregate; Geopolymer mortar; Mix design methodology.

Introduction

Sand, following water, stands as one of the most widely utilized natural resource material globally, reaching a juncture where it is coined as "the new gold." Perpetual extraction of this invaluable material is already causing havoc on both physical and ecological ecosystems of the planet. Projections indicate a striking surge in sand demand across the world, poised to reach 82 billion tons by the year 2060 (Rentier and Cammeraat 2022). Thus, in the realm of construction materials, the scarcity of fine aggregates, particularly river sand, has emerged as a pressing concern in recent years. Fine aggregates play a pivotal role in concrete and mortar production, serving as a vital ingredient that enhances the durability, shrinkage, workability, weight, and strength of concrete structures (Dash et al. 2016). However, overexploitation of river sand has led to a considerable resources depletion, triggering environmental degradation followed by imposition of regulatory restrictions on its extraction. This constraint has propelled the construction industry toward exploring alternative sources of fine aggregates to alleviate the adverse impacts of sand depletion while ensuring concrete and mortar quality and performance. Therefore, the quest for an alternative to fine aggregates has sparked innovation and research endeavors worldwide, driving the discovery and utilization of various materials that exhibit comparable properties to traditional river sand. These alternatives not only offer a sustainable solution to the scarcity issue but also present opportunities to enhance the characteristics of concrete and mortar. From industrial by-products to recycled materials, a plethora of options have been explored to meet the demand of the construction sector while addressing environmental concerns.

Various types of industrial waste materials including, waste foundry sand, steel slag, copper slag, imperial smelting furnace slag, blast furnace slag, coal bottom ash, ferrochrome slag, class F fly ash, recycled glass with graphene oxide, and palm oil clinker, have been employed as a partial substitute for river sand in the production of concrete and mortar (Ambily et al. 2015; Dash et al. 2016; Ganesh Prabhu et al. 2014; Guo et al. 2018; Hosen et al. 2021; Issa Fares et al. 2023; Patra and Mukharjee 2017; Siddique 2003; Singh and Siddique 2015; Tran et al. 2024; Vu Hong Son et al. 2024). The characteristics of concrete and mortar made with the previous alternate fine aggregates are evaluated and compared with controlled concrete and mortar samples made with river sand, to discern differences, if any (Ambily et al. 2015; Dash et al. 2016; Ganesh Prabhu et al. 2014; Guo et al. 2018; Hosen et al. 2021; Issa Fares et al. 2023; Patra and Mukharjee 2017; Siddique 2003; Singh and Siddique 2015). Despite their promise as sustainable alternatives, these industrial by-products exhibited significant disparity in chemical compositions and are largely tied to specific regional waste, leading to inconsistencies in concrete performance. Moreover, concerns regarding potential leaching of heavy metals and long-term durability hinder their widespread acceptance in structural applications.

Alternatively, manufactured sand, produced by crushing rocks, has emerged as a prominent substitute for river sand in concrete production (Pilegis et al. 2016; Kumar 2018). Crushed rock fines, generated by quarry operations, have gained traction as an alternative to river sand. Research has demonstrated the feasibility of utilizing crushed rock fines in concrete production, with optimized mix designs achieving satisfactory performance in terms of strength and durability (Boobalan et al. 2020). Recycled concrete aggregates

[1]Research Scholar, School of Infrastructure, Indian Institute of Technology Bhubaneswar, Odisha 752 050, India. ORCID: https://orcid.org/0000-0002-5883-9066. Email: s22ce09004@iitbbs.ac.in

[2]Scientific Associate, Dept. of Materials, Slovenian National Building and Civil Engineering Institute, Ljubljana, Slovenia. ORCID: https://orcid.org/0000-0003-1658-2466. Email: vesna.zalar@zag.si

[3]Associate Professor, School of Infrastructure, Indian Institute of Technology Bhubaneswar, Odisha 752050, India (corresponding author). ORCID: https://orcid.org/0000-0002-5136-6198. Email: bhrao@iitbbs.ac.in

Note. This manuscript was submitted on March 18, 2025; approved on August 15, 2025No Epub Date. Discussion period open until 0, 0; separate discussions must be submitted for individual papers. This paper is part of the ***Journal of Materials in Civil Engineering***, © ASCE, ISSN 0899-1561.

(RCA), obtained from crushing and processing demolished concrete structures, have exhibited properties suitable for incorporating into the new concrete mixes. Despite challenges related to the variability in quality, advancements in processing techniques and quality control measures have facilitated the widespread utilization of RCA in concrete production (Xiao et al. 2018). Enhanced RCA via washing and thermos-mechanical treatment improved strength, but high energy use and limited scalability hinders its broad adoption (Arulkumar et al. 2025). Quarry dust, a by-product of stone quarrying operations, has been investigated as a potential substitute for river sand in concrete and mortar manufacturing, with optimized mix designs yielding promising results (Rai et al. 2016). It however to be noted that manufactured sand, crushed rock fines, RCA, and quarry dust are ultimately derived from natural resources, raising concerns over the continued depletion of geological reserves. Additionally, their production processes often involve high energy consumption and environmental disruption, limiting their sustainability in the long term. In emerging studies, mortar is being prepared with artificial sand made with fly ash and ground granulated blast furnace slag (Agrawal et al. 2019; Gnanadurai et al. 2021; Sudam et al. 2023). It however to be noted that the sand is made by resorting to hand mixing and crushing methods. Moreover, a notable challenge lies in the irregularity of particle shapes, demanding substantial human resources for their effective utilization and industrial scalability.

Despite numerous prior studies, multitudes of challenges persist in hindering both the traditional applications and future exploration of alternative fine aggregates. Quality control and the composition of alternative sands remain unregulated, leading to disparity in the properties of mortar/concrete prepared with the same substitution ratio. It has been noted that at higher substitution ratios, many alternative sands fail to enhance the mechanical and durability characteristics of mortar, necessitating chemical or mechanical pretreatment prior to their usage, thereby exacerbating costs (Srivastava and Singh 2020).

In recent years, sustainable construction materials have garnered considerable attention due to their potential to mitigate environmental impacts while maintaining structural integrity. Among these materials, fly ash-based geopolymers have popped up as a promising alternative to conventional cementitious systems, owing to their unique chemical compositions and reaction mechanisms. Geopolymers, synthesized by alkali activation of aluminosilicate rich resources such as fly ash, offer notable advantages including reduced carbon emissions, enhanced durability, and maximized waste utilization (Reddy et al. 2016). Moreover, the utilization of fly ash, a by-product of coal combustion, not only addresses waste management concerns but also contributes to resource conservation (Pavithra et al. 2016a).

In the present study, we propose a novel approach to addressing the pressing need for fine aggregates, as a sustainable construction material. We aim to harness the abundantly available resource such as fly ash to develop a viable alternative to traditional river sand in the form of fly ash based sand (FAB sand). FAB sand is prepared by resorting to geopolymerization with cold bonding pelletization technique. The FAB sand mimics the properties of river sand within the particle size range of 4.75–0.075 mm. The novelty of this research lies in the development of fly ash based geopolymer mortar (GPM) using 100% FAB sand, by completely alleviating the use of river sand. GPM cubes made with 100% river sand are used as controlled samples to ascertain the performance of FAB sand as an innovative construction material. No prior research endeavors have been documented to date regarding the formulation of geopolymer mortar utilizing 100% FAB sand as a substitute for conventional fine aggregates (river sand). The development of fly ash sand based GPM, which eliminates the need for cement or river sand, offers a promising path toward ecofriendly infrastructure solutions. The present study represents a novel and ecoconscious solution that holds great promise for the future of construction applications. By embracing innovation and sustainable practices, and aligning with the principles of the circular economy, the construction industry can tackle the challenges of fine aggregate scarcity while paving the way for a greener, more resilient built environment.

Materials and Methodology

Materials

In this study, fly ash (binder solid, BS) was sourced from two distinct locations in Odisha, India. Fly ash 1 (FA1) was obtained from M/s. Vedanta Limited in Lanjigarh, while fly ash 2 (FA2) was sourced from National Thermal Power Corporation Limited in Kaniha. To characterize the particle sizes of FA1 and FA2, gradational analysis was conducted following the guidelines outlined in ASTM D6913/D6913M-17 (ASTM 2017c). Specific gravity (G) and bulk density were measured as per ASTM C128-22 and C29/29M-17a, respectively [ASTM C128-22 (ASTM 2023), ASTM C29/29M-17a (ASTM 2017a)]. Additionally, river sand was procured from a local supplier in Bhubaneswar, Odisha, India. 5

Sodium silicate (Na_2SiO_3) in conjunction with sodium hydroxide (NaOH) was used as alkali activator solutions (AAS) for geopolymerization. Na_2SiO_3 was sourced from Panchi chemicals (Hyderabad) while NaOH pellets (96% purity) were obtained from the Central Drug House. The silicate modulus of Na_2SiO_3 solution is 3.1 ($SiO_2 = 28.24\%$, $Na_2O = 9.10\%$, $H_2O = 62.66\%$). NaOH solution was prepared at molarities ranging from 2 to 14. The reaction between water and NaOH is exothermic, releasing a significant amount of heat. Therefore, the prepared NaOH solution was left in undisturbed condition for 24 h to dissipate the heat. The G of NaOH solution prepared at 2, 4, 6, 8, 10, 12 and 14 M was measured as 1.12, 1.18, 1.24, 1.26, 1.32, 1.36 and 1.39, respectively. Alternatively, the G of Na_2SiO_3 was measured to be 1.45.

Preparation of Fly Ash Based Sand (FAB sand)

The process of making FAB sand using geopolymerization and cold bonding pelletization, as outlined in this study, follows the procedure established by Sekhar and Rao (Sekhar and Rao 2024a).
6 Fig. 1 illustrates the process of developing FAB sand, showing geopolymerization, pelletization and cold bonding. A custom-made disc pelletizer equipment was employed for the preparation of sand sized fractions using fly ash alone as a precursor material. The pelletization process is associated with aggregation of moistened particles within a rotating drum (Baykal and Döven 2000). This aggregation or bonding relies heavily on geopolymer technology, which initiates geopolymerization, an inorganic polymeric technique. Geopolymerization transforms finely pulverized particles of aluminosilicate-rich precursor material into a hardened substance upon the addition of alkali solutions, forming a robust 3-D network of linkages (Pavithra et al. 2016b). Employing cold bonding, where temperature typically remain below 100°C (Liu et al. 2023), facilitates the curing of the agglomerated sand particles, a methodology adhered in this study.

Recently, Sekhar and Rao (2025) demonstrated that the median particle size of fly ash also affects the gradation of FAB sand. Hence, the present study utilizes two variety of fly ashes (FA1 and FA2) to produce FAB sand (FABS1 and FABS2). Sand fractions prepared with FA1 and FA2 are herein named as FABS1 and FABS2, emphasizing their distinct origins and characteristics, as discussed in section 2.1. FABS1 and FABS2 were prepared by 7 a precise alteration of NaOH molarities from 2 to 14 for FABS1

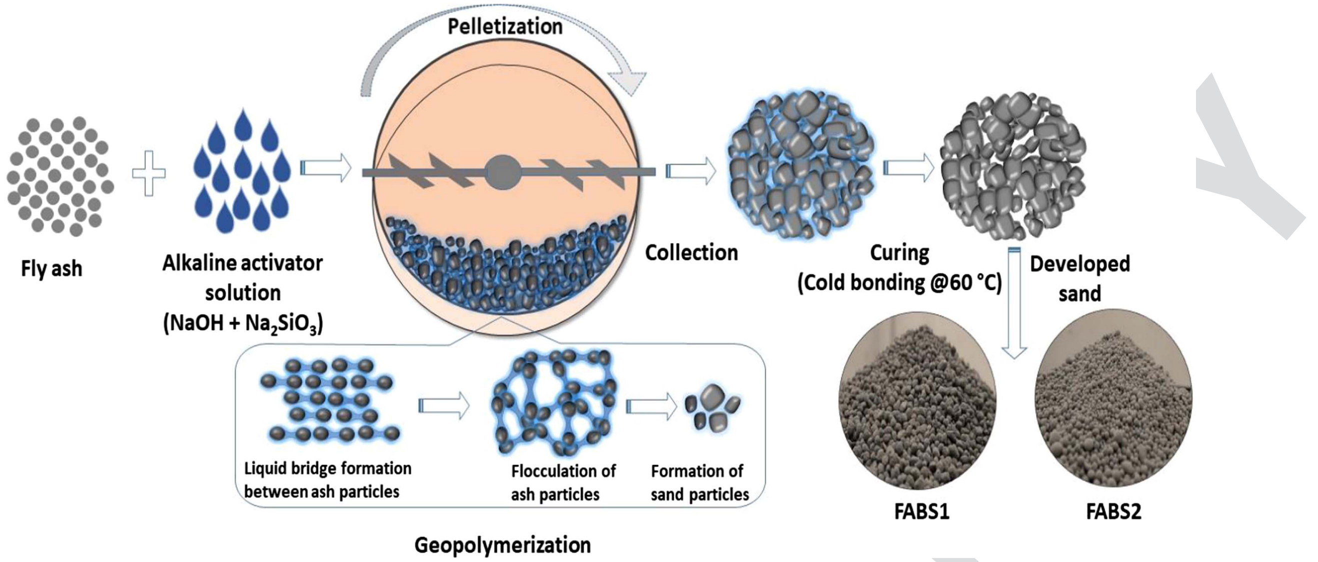

Fig. 1. Process of developing FAB sand.

and 6 to 12 for FABS2, ensuring a diverse array of compositions for optimal performance. After extensive experimentations, the production parameters that would aid in acquiring the desired gradation of FABS1 were meticulously defined as: pelletizer tilt angle of 50 degree, duration of 30 minutes, speed of 15 rpm and AAS to BS ratio of 0.34. Similarly, the production parameters for achieving FABS2 were defined as: pelletizer tilt angle of 50 degree, duration of 15 minutes, speed of 10 rpm and AAS to BS ratio of 0.10.

Development of Fly Ash Based Geopolymer Mortar (GPM)

Fly ash based GPM cubes were prepared employing two variants of 100% FAB sand (i.e., FABS1 and FABS2) as well as 100% river sand as a controlled material. The development of GPM involved three key stages: mix design methodology, cube casting, and characterization of cubes.

Mix Design Methodology

The present study adopts a performance-driven mix design methodology that incorporates the specific gravity of all raw materials, ensuring volumetric consistency and optimal packing. Based on established geopolymer concrete (GPC) mix design frameworks proposed in the literature, the method is innovatively adapted for GPM, precisely adjusting proportions to formulate GPM cubes (Pavithra et al. 2016a; Reddy et al. 2018). Fig. 2 illustrates the multifaceted process of developing GPM mix design and elucidates each sequential step. Based on numerous trials, AAS/BS ratio and $Na_2SiO_3/NaOH$ ratio were fixed at 0.5 and 1.5 for making the GPM cubes using river sand, FABS1, and FABS2, respectively. Moreover, this selection aligns with prior findings by Ray et al. (2025) and Pavithra et al. (2016b), who identified similar optimal ratios for fly ash based GPM systems. River sand served as a controlled material, allowing for the assessment of the performance of FABS1 and FABS2. Three distinct sets of GPM cubes were cast. One mix utilized only river sand while in other two, FAB sand was fully (100%) substituted for river sand. The FAB sand used was made at different molarities of NaOH ranging from 2 to 14 for FABS1 and 6 to 12 for FABS2. Such consideration demonstrates the versatility and adaptability of the developed FAB sand as a fine aggregate. For GPM mixes with river sand, NaOH molarity is varied as 8, 10, 12, and 14, to investigate its influence on mechanical

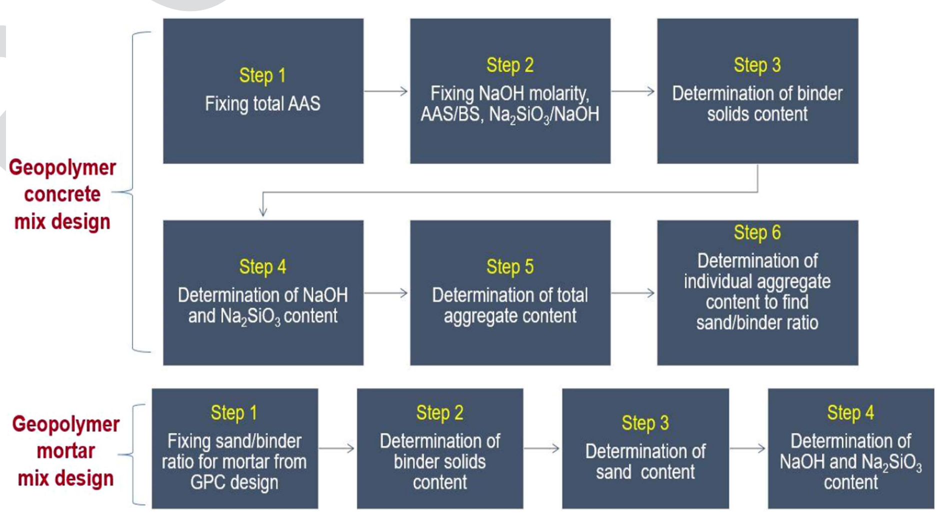

Fig. 2. Mix design methodology for developing geopolymer mortar and concrete.

Table 1. Sample calculations for the mix design of GPC to determine sand to binder ratio

	Parameter	Notation	Description	Quantity	Unit
T1:1	Parameter	Notation	Description	Quantity	Unit
T1:2	Alkaline Activator Solution	AAS	Based on workability and economic criteria	200	kg/m^3
T1:3	AAS to Binder Solids ratio	AAS/BS	Fixed as per strength requirements	0.5	—
T1:4	Molarity of NaOH	M		10	M
T1:5	$Na_2SiO_3/NaOH$ ratio	R	Fixed based on maximum compressive strength	1.5	—
T1:6	Binder solid Content	B_C	AAS/(AAS/BS)	400	kg/m^3
T1:7	Mass of NaOH	M_{NaOH}	Mass of AAS/$(1+R)$	80	kg/m^3
T1:8	Mass of Na_2SiO_3	$M_{Na_2SiO_3}$	Mass of AAS—Mass of NaOH	120	kg/m^3
T1:9	Volume of entrapped air	V_a	Assuming	2	%
T1:10	Volume of binder solids	V_B	B_C/G of B_C	0.185	m^3
T1:11	Volume of sodium silicate	$V_{Na_2SiO_3}$	$M_{Na_2SiO_3}$/G of Na_2SiO_3	0.0827	m^3
T1:12	Volume of sodium hydroxide	V_{NaOH}	M_{NaOH}/G of NaOH	0.0606	m^3
T1:13	Total Combined Aggregate	V_{TA}	(1-va)—$(V_B + V_{Na_2SiO_3} + V_{NaOH})$	0.652	m^3
T1:14	Sand for concrete	M_{sand}	$V_{TA} \times G_{sand} \times$ percentage of sand in total aggregate (38) $\times$ 1000	651	kg/m^3
T1:15	Ratio of sand/binder in concrete	M_{sand}/B_C	Ratio of sand to binder in concrete	1.628	—

Table 2. Sample calculations for the mix design of GPM

	Parameter	Notation	Description	Quantity	Unit
T2:1	Parameter	Notation	Description	Quantity	Unit
T2:2	Binder solid content for mortar	M_{BS}	$2000/(1+(M_{sand}/B_C))$	760.828	kg/m^3
T2:3	Sand for mortar	M_{FA}	2000—M_{BS}	1239.17	kg/m^3
T2:4	AAS content for mortar	M_{AAS}	$M_{AAS} = M_{BS} \times AAS/BS$	380.4	kg/m^3
T2:5	Mass of NaOH	M_{NaOH}	$M_{NaOH} = M_{AAS}/(R+1)$	152.17	kg/m^3
T2:6	Mass of Na_2SiO_3	$M_{Na_2SiO_3}$	$M_{Na_2SiO_3} = R \times M_{NaOH}$	228.25	kg/m^3

performance. Based on the integrated evaluation of strength performance and economic feasibility, the optimal NaOH molarities were subsequently selected for GPM, incorporating FABS1 and FABS2. A detail sample calculations of quantities for preparing GPM with river sand obtained from the GPC mix design is given in Tables 1 and 2.

GPM Cube Casting

The process of cube casting primarily comprises of mixing, casting, and curing sequences. Mixing encompasses the dry mixing of raw materials such as fly ash (FA2) and sand (FAB or river sand) for 3 min to ensure uniformity. After the dry mixing, NaOH and Na_2SiO_3 solutions were added and the contents were blended for an additional 4 min. The mixture was then transferred to the standard-sized cube casting molds (each with a side length of 70.6 mm) according to IS: 4031 (Part 6) standard (BIS 2006). Tampering and simultaneous compaction was accentuated using a vibrating table. The surface was then carefully smoothed to ensure a uniform finish. Casts were wrapped with polythene sheet to prevent moisture loss, and subjected to elevated curing temperature at 60 and 80°C for 24 h. After cooling to room temperature, GPM samples were demolded and cured at ambient conditions (i.e., 27 ± 1°C) for 7, 14, and 28 days. Fig. 3 delineates the GPM mixing sequence, providing a comprehensive visual guide to the process.

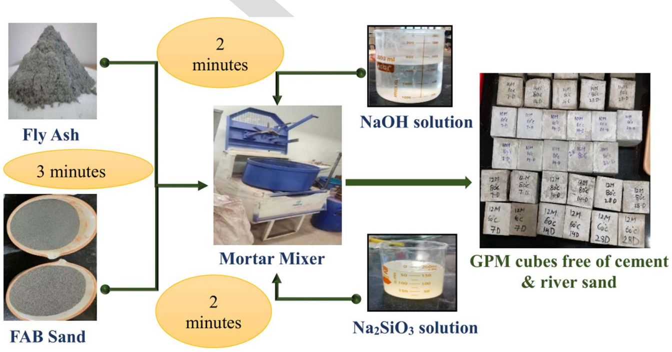

F3:1 **Fig. 3.** Process of preparing geopolymer mortar.

Characterization of GPM Cubes

The compressive strength of GPM cubes was measured after 7, 14 and 28 days of curing with the help of HEICO (HLM 592) press boasting 3000 kN capacity with 0.2 MPa accuracy machine. Tests adhere to loading rate of 35 N/mm^2/minute as per the ASTM C109 guidelines [ASTM C109/C109-20a (ASTM 2020)]. The maximum compressive load at failure was recorded for each cube. The compressive strength was calculated by dividing the cross-sectional area (49.84 cm^2). Each result represented the average of three measurements. Water absorption significantly influences the durability, quality, strength, and longevity of structures; therefore, it was measured on the samples after 28 days of curing. GPM specimens were immersed in water for 24 ± 1 h as per ASTM 1403 standard [ASTM 1403-22a (ASTM 2022)]. Each set of three replicate specimens was considered representative, with their average indicating the water absorption. The correlation between 28th day compressive strength, water absorption, and density of GPM cubes from FAB sand was assessed.

Morphological and Mineralogical Analysis

Before conducting scanning electron microscope (SEM) analysis on FA, FAB sand, river sand, and GPM cubes to observe changes in particle morphology, samples were sputtered with gold coat using a Q150R ES sputter coater. The morphological features and semi quantitative chemical analysis of samples (i.e., FA, FAB sand, river sand, and GPM) were performed using a MERLIN compact field emission SEM (ZEISS FEI Quanta 25, Berlin) coupled with energy dispersive x-ray spectroscopy (EDS) analysis.

The phase compositions of FA, FAB sand, river sand, and GPM cubes were defined by X-ray diffraction (XRD) analysis, a D8 advance x-ray powder diffractometer equipped with a LYNXEYE detector, and copper (Cu-Kα) radiation. Samples were scanned at 40 mA current and 30 kV voltage, in a range from 5°–90° of 2θ, with a step size of 0.2. The X'Pert High Score Plus software was utilized to characterize the mineral phases. Prior to analysis, specimens were finely ground and subjected to oven drying at 95°C–105°C for 24 ± 1 h.

Leaching Analysis

In order to assess the environmental acceptability of GPM cubes developed with FAB sand, toxicity characteristic leaching procedure

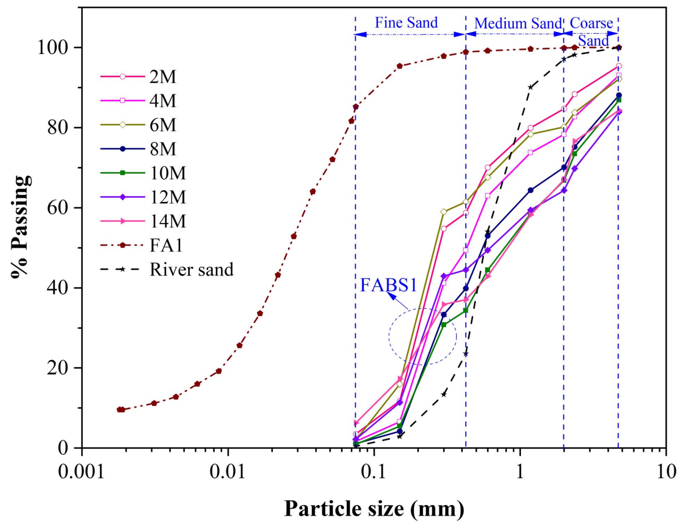

Fig. 4. Gradation curves of FABS1 for varying NaOH molarity.

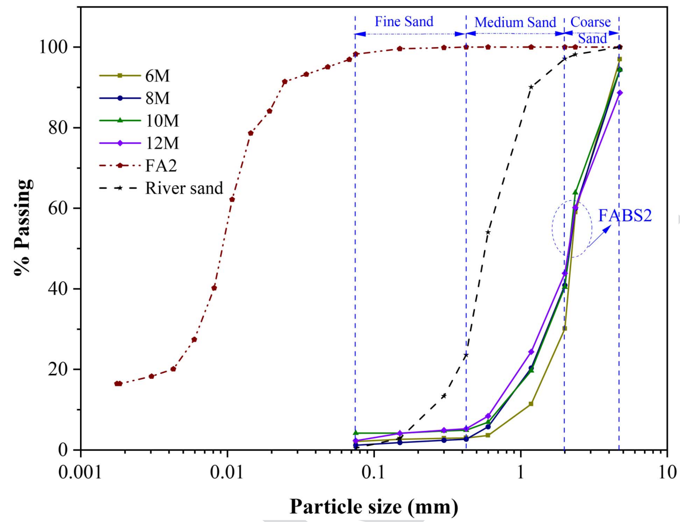

Fig. 5. Gradation curves of FABS2 for varying NaOH molarity.

(TCLP) was applied as per the protocol outlined in USEPA Method 1311 [US Environmental Protection Agency 1311 (USEPA 1992)]. Potentially toxic elements (PTEs) including arsenic (As), cadmium (Cd), chromium (Cr), copper (Cu), lead (Pb), mercury (Hg), manganese (Mn), nickel (Ni), and zinc (Zn) were measured by ICP flame photometer with optical spectroscopy. Additionally, concentrations of calcium (Ca), iron (Fe), magnesium (Mg), potassium (K), and sodium (Na) were determined. Alongside leachability of PTEs in FA1, FA2, FABS1, and FABS2 were also analyzed. The concentrations of leached PTEs were compared with the limiting values set by the Hazardous and Other Wastes (Management and Transboundary Movement) Rules, 2016, established by the Ministry of Environment, Forest, and Climate Change (MoEF&CC), Government of India (MEFCC 2019) as well as the USEPA guidelines (USEPA 2004).

Results and Discussion

Characterization of Materials

Figs. 4 and 5 present the gradation curves of FA and FAB sands. Gradation curves of FABS1 and FABS2 are presented as a function of NaOH molarity. For a comparison with the reference aggregate, the gradation curve of river sand is also shown in Figs. 4 and 5. The results clearly show that FAB sand gradation curves align well with the particle size distribution of river sand.

Particle size distribution curves in Figs. 4 and 5, show that FA1 comprises 15%, 75%, and 10% of sand, silt, and clay size fractions while FA2 consists of 2%, 81%, and 17% of sand, silt, and clay size fractions. The fly ash gradation curves clearly demonstrate the prevalence of silt sized fractions. The D_{50} of FA1 and FA2 is measured as 25 and 9 μm, exhibiting FA1 as a coarser grained than FA2. The specific gravity of FA1 and FA2 is determined as 2.13 and 2.16, respectively. Whereas, the loose and rodded bulk density (kg/m^3) is measured as 894 and 1076 for FA1, and 819 and 1042 for FA2.

A clear gap between the gradation curves of FA and FAB sand shows that sand can successfully be produced using fly ash as a resource material through geopolymerization with cold bonded pelletization technique. Figs. 4 and 5 clearly shows the composition of river sand, highlighting a blend of 3% coarse (4.75–2 mm), 74% medium (2–0.425 mm), and 23% finer (0.425–0.075 mm) fractions. Conversely, FABS1 yielded coarse, medium, and fine fractions in the range of 16%–36%, 24%–29% and 35%–57% while FABS2 produced these fractions in the range of 40%–50%, 25%–35% and 6%–10%. It can also be observed from Figs. 4 and 5 that 100% FA is converted into sand (~90%) and gravel (~10%). The variation in percent fractions of FAB sand is attributed to differences in the median particle of FAs, molarity of NaOH and AAS/BS ratio. FA2, with a lower D_{50} than FA1, requires a lower AAS/BS ratio for producing FABS2, compared to FABS1. Figs. 4 and 5 also show that as the molarity of NaOH increases, the fraction of the coarser particles also increases.

Table 3. Comparison of properties of river sand and FAB sand

Parameter	River sand	FABS1	FABS2
Specific gravity	2.63	1.9–2.2	1.8–2.1
Water absorption (%)	1.4–2.8	9–17	12–22
Loose density (kg/m^3)	1546	820-900	780-830
Rodded density (kg/m^3)	1620	930-1000	850-910
Compacted density (kg/m^3)	1726	1020-1090	920-1010
pH	8.5	10–12.5	9.5–11.5

The value of specific gravity, water absorption, density (loose, rodded, and compacted), and pH measured for river sand, FABS1 and FABS2 is listed in Table 3. The higher water absorption of FAB sand in comparison to river sand can be attributed to the presence of voids within the grains of FAB sand. These voids might have formed during the agglomeration process of ash particles (Sekhar and Rao 2024a, b). Based on the measured density values of FAB sand and the ASTM C330 standard [ASTM C330/C330M-17a (ASTM 2017a)], it can be classified as a lightweight aggregate, with a density below 1120 kg/m^3 threshold. pH of river sand, FABS1 and FABS2 are measured as 8.5, 10–12.5 and 9.5–11.5, respectively.

Fig. 6 illustrates the aggregate crushing strength (%) of FABS1, FABS2 and river sand. For FABS1, prepared at molarities ranging from 2 to 14, the crushing value decreased from $12.3 \pm 0.5\%$ to $5.1 \pm 0.4\%$, indicating a notable enhancement in mechanical resistance with increasing NaOH concentration. Similarly, FABS2, developed from 6 to 12 M, exhibited crushing values between $17.5 \pm 0.7\%$ and $11.5 \pm 0.5\%$. In comparison, river sand showed a crushing value of $5.7 \pm 0.4\%$. According to IS 2386 Part 4 (BIS 1963), fine aggregates used in concrete should have an aggregate crushing value below 30%. Notably, the developed FAB sands fall

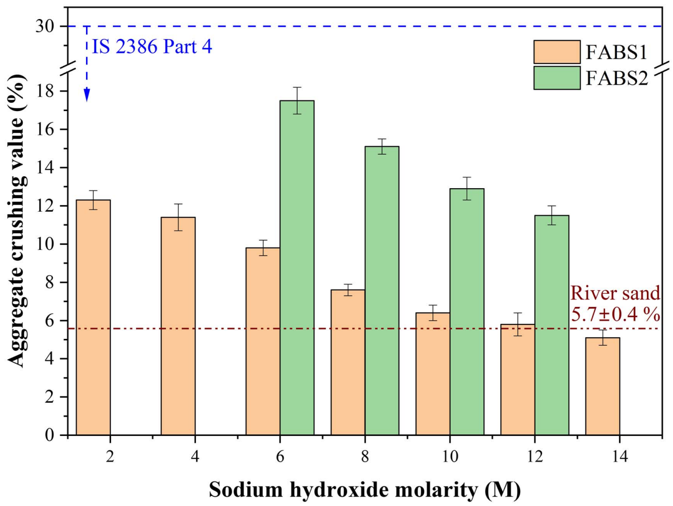

Fig. 6. Aggregate crushing value of FAB and river sands.

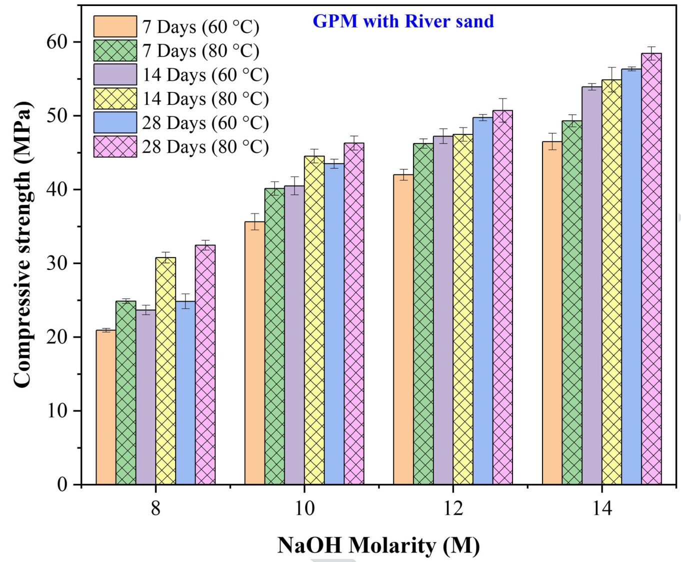

Fig. 7. Compressive strength of GPM cubes made with 100% river sand. (control sample.)

well within this limit, demonstrating their potential as structurally viable alternatives to river sand in mortar and concrete applications.

The characterization results emphasize the comparability of FAB sand to river sand, affirming its suitability as an alternative fine aggregate for the construction purpose.

Fresh Properties of GPM

The workability of developed GPM is assessed using flow tests, as per ASTM C1437-15 (ASTM 2015) and IS 4031 Part 7 (BIS 1988), targeting a spread diameter of 110 ± 5 mm (standard consistency). The water absorption of FABS1 and FABS2 is measured as 9–17% and 12–22%, which is higher than river sand (1.4–2.8%). The values measured are listed in Table 3. To alleviate the effect of water absorption, fine aggregates are first brought to the surface-saturated state followed by the addition of naphthalene-based superplasticizer (1–15% by weight of fly ash) to restore flow without altering the water-to-binder ratio (Nath and Sarker 2015; Pratap et al. 2024).

The superplasticizer demand in GPM increased consistently with the molarity of NaOH, particularly when using FABS1 and FABS2, due to their higher water absorption compared to river sand. For FABS1, the required superplasticizer dosage (%) to achieve the targeted flow is 1.0, 2.5, 4.0, 6.5, 8.8, 10.9, and 14.6% at NaOH molarities of 2, 4, 6, 8, 10, 12, and 14, respectively. For FABS2, the dosage (%) needed are 5.8, 9.2, 11.6, and 13.8% for 6, 8, 10, and 12 M, respectively. In contrast, mortar mixes using river sand, which has significantly lower water absorption, required much lower superplasticizer dosage of 1.5%, 2.1%, 3.5%, and 4.6% for NaOH molarities of 8, 10, 12, and 14, respectively. The superplasticizer content pertinent to river sand mortar is consistent with the literature studies (Duxson et al. 2007; Paul 2022; Anudeep et al. 2024). This approach of surface saturating and optimizing superplasticizer dosage has achieved the requisite flowability, maintaining a balance between fresh properties and mechanical integrity.

Compressive Strength Results

Fig. 7 shows the compressive strength results of GPM made with 100% river sand as a control sample at various NaOH molarities of 8, 10, 12, and 14. The bar chart illustrates the changes in strength during elevated curing at 60 and 80 degrees. The 28th day compressive strength corresponding to 8, 10, 12, 14 M is measured as 24.85 ± 1.0, 43.49 ± 0.6, 49.74 ± 0.4, 56.34 ± 0.3 MPa at 60°C and 32.45 ± 0.7, 46.3 ± 0.9, 50.71 ± 1.6, 58.44 ± 0.9 MPa at 80°C elevated temperature curing. Fig. 7 shows that as the molarity of sodium hydroxide (8–14) increases so does the compressive strength. This enhancement can be attributed to the improved dissolution of aluminosilicates of fly ash at higher alkaline concentrations. Elevated NaOH molarity boosts the solubility of silicate and aluminate species, which in turn accelerates the geopolymerization reaction and results in a denser, more interconnected polymeric matrix. An increase in compressive strength with curing temperature (60°C–80°C) and curing age (7–28 days) can also be noticed from Fig. 7. Higher curing temperatures accelerate the geopolymerization process by enhancing the mobility of reactive species, promoting faster evaporation of water, and intensifying the rate of polycondensation reactions. This results in a denser, more compact matrix and quicker strength development. Similarly, longer curing durations allow the geopolymer network to further develop and refine over time, improving internal bonding and structural integrity. Similar results are reported by Pavithra et al. (2016b) on fly ash based GPM cubes.

According to Fig. 7, 28th day compressive strength of 46.3 MPa can be developed when using 10 M NaOH solution. To derive GPM of equivalent strength, cubes are made with 100% FAB sand using the same mix design, sample preparation, and curing process that adopted for 10 M NaOH solution. This enables a direct comparison of FAB sand performance vis-à-vis with river sand. While higher molarity NaOH solutions typically yield greater strength, they also significantly increase the overall cost of the mortar production. For this reason, the development of GPM using FAB sand is limited to 10 M concentration, balancing strength performance with cost efficiency.

Fig. 8 shows the compressive strength results of GPM from 100% FABS1 made at various NaOH molarities of 2, 4, 6, 8, 10, 12, and 14. The 28 days compressive strength of cubes corresponding to these molarities is determined as 30.7 ± 0.8, 33.6 ± 1.6, 40.6 ± 1.2, 42.6 ± 0.9, 43.8 ± 1.1, 33.6 ± 0.4, 27.2 ± 0.5 MPa at 60°C and 31.2 ± 0.8, 37.6 ± 0.4, 41.82 ± 0.8, 43.8 ± 0.6, 45.1 ± 0.6, 34.3 ± 1.5, 29.0 ± 1.2 MPa at 80°C of elevated temperature curing. Contrary to river sand, the compressive strength of GPM cubes made with FABS1 increased up to 10 M NaOH concentration and decreased thereafter. This may be attributed to enhanced precipitation of aluminosilicate gels on account for the

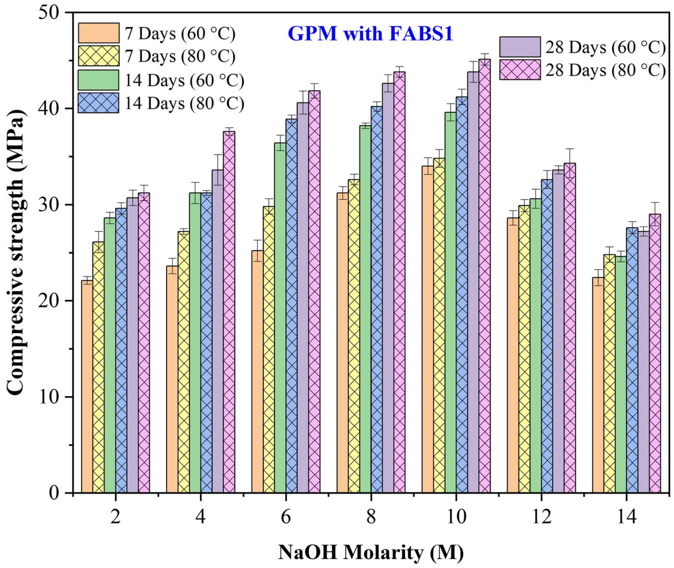

F8:1 **Fig. 8.** Compressive strength of GPM cubes made with 100% FABS1.

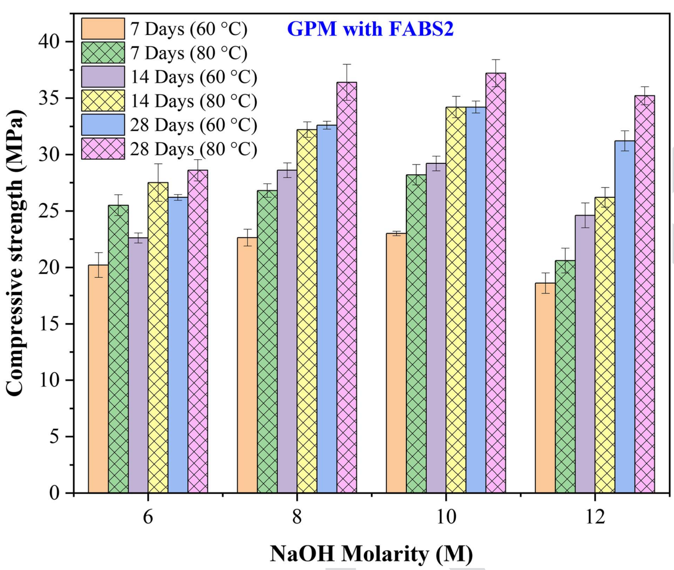

F9:1 **Fig. 9.** Compressive strength of GPM cubes made with 100% FABS2.

excess NaOH solution in the system, leading to rapid hardening besides hindering the formation of other geopolymeric precursors (Lee and Van Deventer 2002). It can also be noticed that strength increased with curing age and temperature. Thus, it can be stated that GPM from 10 M FABS1 attained a noteworthy compressive strength of 45.1 MPa, closely aligning with the target strength of 46.3 MPa, demonstrating the efficiency of FAB sand as a potential replacement for river sand.

Fig. 9 shows the compressive strength results of GPM when using 100% FABS2 developed at various NaOH molarities (6, 8, 10, and 12). The 28 days compressive strength corresponding to these molarities is measured as 26.2 ± 0.3, 32.6 ± 0.4, 34.2 ± 0.5, 31.2 ± 0.9 MPa at 60°C and 28.6 ± 0.9, 36.4 ± 1.6, 37.2 ± 1.2, 35.2 ± 0.8 MPa at 80°C. Similar to FABS1, the compressive strength of GPM from FABS2 increased up to 10 M NaOH concentration and then decreased. The maximum compressive strength of 37.2 MPa is measured for FABS2, which is slightly lesser in comparison to FABS1 performance. The lower strength value may be attributed to the lower AAS/BS ratio of 0.1 used for producing FABS2, compared to 0.34 for FABS1. Alike results presented in Figs. 7 and 8, it can be observed from Fig. 9 that strength increased with an increase in curing age and temperature.

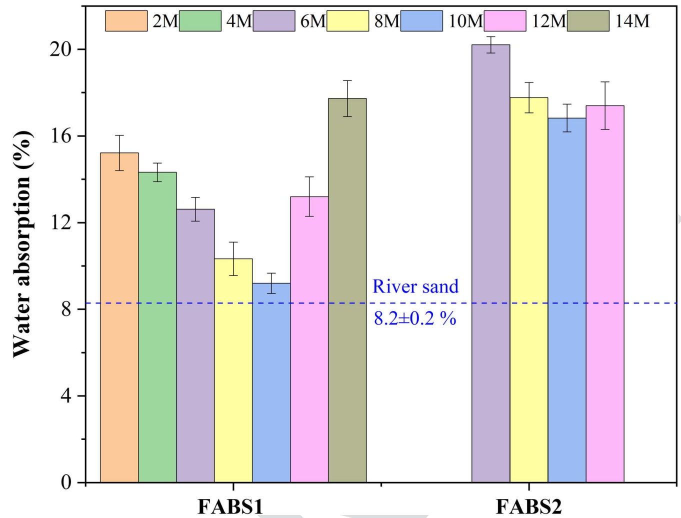

Fig. 10. Water absorption of GPM cubes made with 100% River and FAB sands. F10:1

Water Absorption and Density Results

Fig. 10 shows the water absorption properties of GPM made from 100% river sand and 100% FAB sand. The results illustrate that cubes made solely of river sand absorb $8.2 \pm 0.2\%$ of water while that of FABS1 absorb 9%–17% across different molarities. An 8% difference in water absorption can be witnessed among GPM cubes made with FABS1. GPM from 10 M FABS1 yielded the lowest water absorption of $9.2 \pm 0.4\%$. Higher compressive strength values are also observed for the same combination (Fig. 8). Water absorption decreased with an increase in NaOH molarity up to 10 M and then descended with further increase in molarity. Alternatively, the water absorption decreased from 20% to 17% for cubes made with 100% FABS2, as the molarity of NaOH increased. Cubes composed of FABS2 exhibited a slightly higher water absorption compared to FABS1 samples. This may be attributed to FABS2 possessing a higher water absorption capacity than both FABS1 and river sand, as shown in Table 3.

Additionally, densities of developed GPM with FAB and river sand are measured after 28 days of curing, as presented in Fig. 11. The density of GPM with river sand is measured as ~2,050 kg/m^3. According to Zailani et al. (2024), the density of FA based GPM with river sand typically falls within 2,000 to 2,230 kg/m^3, depending upon the binder to sand ratio. Conversely, for FABS1, the density ranged from 1656 to 1,753 kg/m^3, and for FABS2, it ranged from 1,632 to 1,691 kg/m^3. Romero et al. (2023) have categorized mortars with an oven dry density under 2,000 kg/m^3 as lightweight mortars, offering their potential benefits for use in both structural and nonstructural applications. Thus, the measured densities indicate that FAB sand is an optimal choice for producing GPM cubes for lightweight construction, effectively reducing the dead load and enhancing design flexibility where weight reduction is crucial (Kumar et al. 2023).

Correlations for Water Absorption and Density versus Compressive Strength

Based on the results obtained from strength and water absorption tests, an effort is further made to correlate various properties, as shown in Fig. 12. The input data for Fig. 12 is derived from

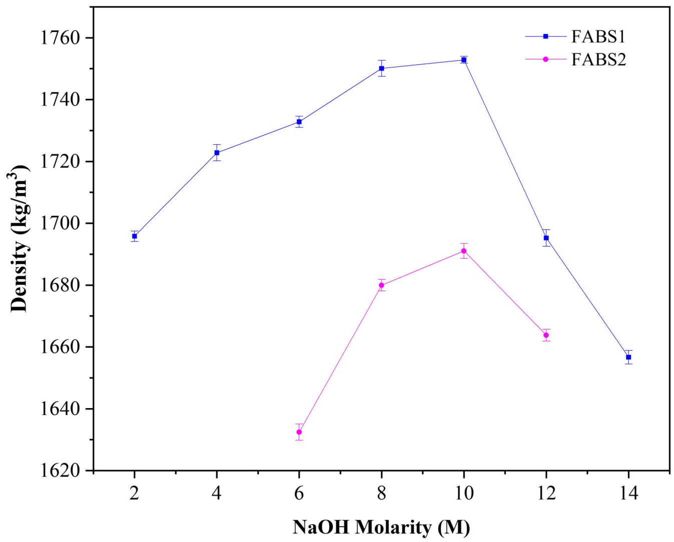

Fig. 11. Density of GPM cubes made with 100% FAB sand.

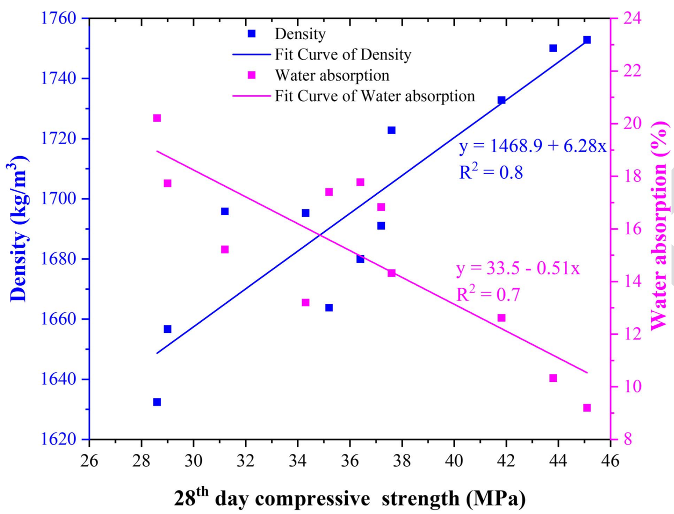

Fig. 12. Correlations for water absorption and density versus compressive strength of GPM cubes made with FAB sand.

Figs. 8 and 9 corresponding to GPM exhibiting maximum compressive strength after curing for 28 days at 80°C. A linear fit model is employed to correlate density and water absorption with compressive strength, as depicted in Fig. 12. Correlations reveal an inverse linear relationship for water absorption versus compressive strength and a linear relationship for density versus compressive strength. A regression coefficient (R^2) of 0.8 for density versus strength and 0.7 for water absorption versus strength is obtained from the trend lines. Fig. 12 shows that as the density increases, so does compressive strength. Conversely, samples that showed higher compressive strength exhibited lower water absorption. Mechanistically, increased density typically reflects a more compact and homogeneous matrix with reduced porosity and fewer microstructural flaws, which enhances the compressive strength of GPM. Conversely, higher water absorption generally indicates greater pore connectivity and void content, which can act as stress concentrators, compromising mechanical integrity. These relationships suggest that optimizing mix design to reduce porosity and increase matrix compactness can significantly enhance strength and decrease water absorption of GPM. These findings align well with the linear regression model proposed by Gupta and Siddique (2020) and Pratap et al. (2024), reinforcing the observed correlations for density and water absorption versus compressive strength.

Morphological and Mineralogical Analysis

Fig. 13 presents micrographs of FA, FAB sand, river sand, together with GPM made with river sand and FAB sand. As depicted in Figs. 13(a and b), FA1 and FA2 particles are predominantly spherical and well-rounded shape, reflecting the typical morphological features of coal combusted fly ash glassy spherules. River sand particles, as seen in Fig. 13(c), are predominantly found in low spherical angular morphology. However, FAB sand exhibits a distinct blend of angular and rounded grains [Figs. 13(d–g)]. A close comparison of Figs. 13(a and b) (i.e., FA alone) with Figs. 13(d and f) (FAB sand) highlights the agglomeration of FA particles, which resulted in FAB sand featuring a wider range of particle size distribution. At lower magnifications [Figs. 13(d and f)], FABS2 grains appear less porous, with almost no visible large voids and a more uniformly round shape grains. However, deeper insights of higher magnification images [Figs. 13(e and f)] reveal that FABS1 contains a greater quantity of binder material, interconnecting the ash relics into a more consolidated structure. In contrast, Fig. 13(g) shows that the ash particles in FABS2 are primarily agglomerated and not evidently surrounded by a continuous binder matrix. Most of the pores in FABS1 are not interconnected, rather they are interconnected only to a limited extent, compared to FABS2. This could be linked to higher water absorption and lower density of FABS2 than FABS1, as presented in Table 3. However, the resemblance in terms of size and shape between the morphological features of river and FAB sand suggests that the sand produced in this study can serve as a viable substitute for the conventional river sand in construction applications.

Figs. 13(h–m) shows SEM images of GPM chunks made with river sand, FABS1, and FABS2. Figs. 13(h, j, and l) depicts the surface morphology of unpolished GPM samples while Figs. 13 (i, k, and m) show their polished counterparts, offering a comparative insight into texture and structural differences. Micrographs in Figs. 13(h–i) reveal interspersed river and FAB sand grains within GPM cubes. These images also show the developed matrix accompanied by gel formations resulting from geopolymerization. The micrograph in Fig. 13(l) shows a greater presence of voids compared to Fig. 13(j). This feature can be correlated to GPM made with FABS2, exhibiting higher water absorption, which is likely due to greater pore connectivity within the matrix, and also results in lower density compared to GPM made with FABS1, as shown in Figs. 10 and 11. These interconnected voids not only reduce the materials resistance to moisture ingress but also be linked to lower compressive strength of GPM made with FABS2 (Fig. 9) compared to those with FABS1 (Fig. 8).

Furthermore, Fig. 13(i) highlight the interfacial transition zone (ITZ) between the matrix and natural river sand, and Figs. 13(k and m) depicts the ITZ between the matrix and FAB sands. Figs. 13(i, k, and m) show that the geopolymer matrix is in close contact with the aggregate surface in all three samples. No micro cracks or porous area can be noticed in ITZs. The difference between FABS1 and FABS2 is evident, as different raw ashes are used in the preparation of aggregates. While the grains of FABS1 are clearly distinguishable within the geopolymer mortar matrix, the FABS2 grains appear more intermixed with the matrix. Due to the lower matrix density and similar absorption coefficient of FABS2, the ITZ boundaries are less clearly defined. In some cases, it is difficult to determine whether the observed zoned regions belong to the aggregate grains or represent areas of higher matrix density. Additionally, in the FABS2 mortar, fine cracks are visible. Nonetheless, Figs. 13(h–m)

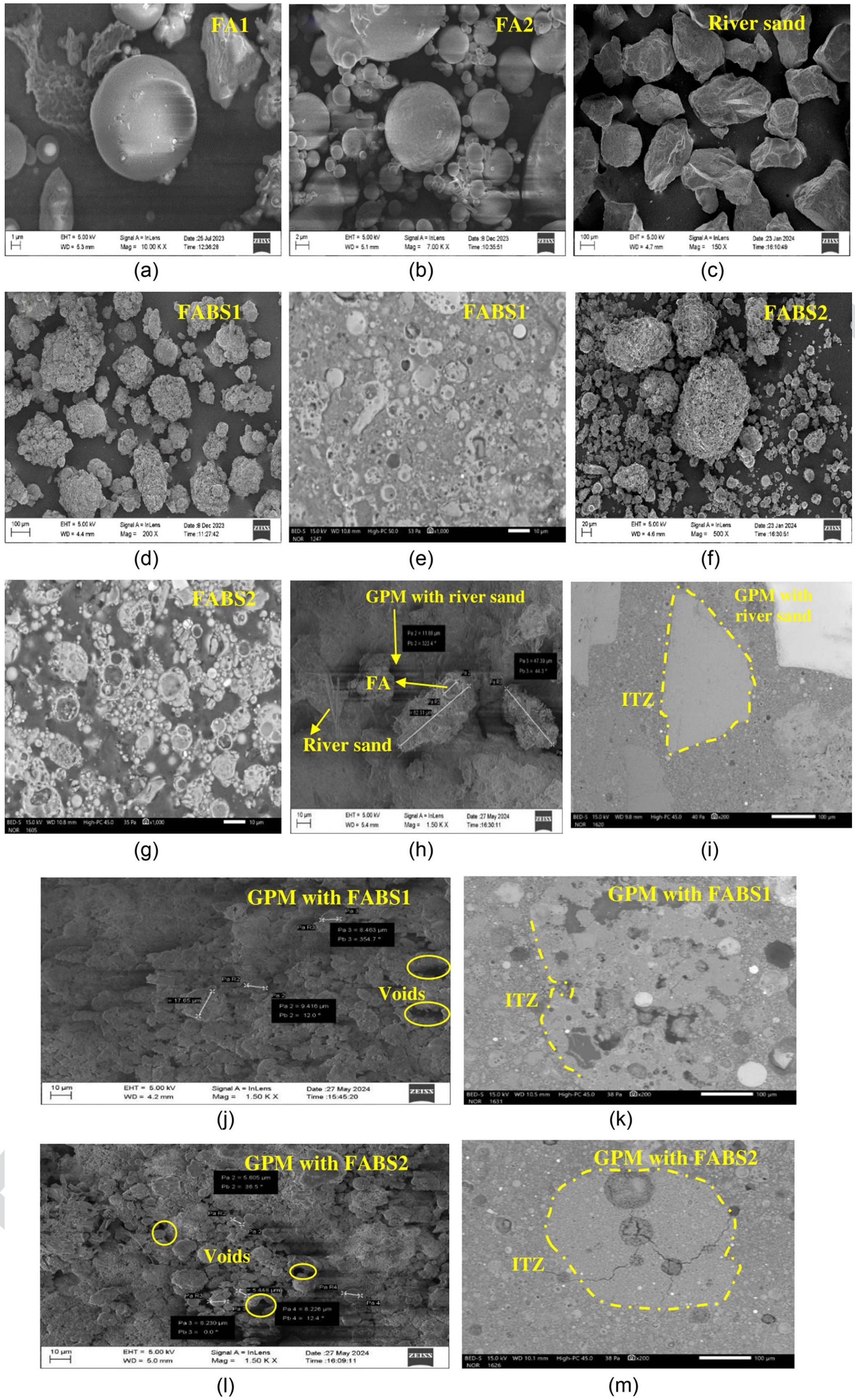

Fig. 13. SEM images of (a) FA1; (b) FA2; (c) River sand; (d and e) FABS1; (f and g) FABS2; and GPM made with (h and i) river sand; (j and k) FABS1; and (l and m) FABS2.

illustrate the formations of very good bonding of FAB sand particles with GPM matrix, aided by gel formations.

EDS analysis reveal that FAs, FAB sands, and GPM from FAB sands consist mostly of Si and Al. In comparison to FA2, its aggregate and mortar samples, FA1 (and its aggregate and mortar) contains relatively higher quantities of Fe and Ca (Table 4). The major elements in river sand include Si and Al. In contrast, GPM cubes made with river sand exhibited a broader range of elements

Table 4. Elemental compositions of fly ash, FAB sand, river sand, and GPM samples

Material	Element (% by weight)								
	Na	Mg	Al	Si	K	Ca	Ti	Fe	Si/Al
FA1	0.15	2.10	30.09	49.41	2.35	5.54	3.72	6.43	1.64
FA2	0.26	0.48	30.76	60.28	4.32	0.3	1.48	2.12	1.96
River sand	—	0.10	9.95	88.14	—	—	—	1.81	8.86
FABS1	7.86	0.78	24.39	51.70	1.27	5.61	2.31	6.08	2.12
FABS2	2.18	0.76	25.59	61.59	2.89	2.83	1.19	2.77	2.41
GPM with river sand	9.0	0.48	20.36	59.41	2.1	0.96	3.59	3.99	2.92
GPM with FABS1	8.15	0.42	23.11	59.60	2.0	1.03	1.87	3.81	2.58
GPM with FABS2	4.72	0.62	25.24	62.06	2.36	1.2	1.68	2.12	2.46

including Si, Al, Na, Ca, Fe, and Mg. This expanded elemental compositions may be attributed to the incorporation of both FA and river sand in the control GPM mix. FAB sand and GPM cubes made with FAB sand exhibited a notable decrease in the weight percentages of Al, Fe, and Ca, simultaneously showing an increase in the weight percentages of Si and Na, as a result of the geopolymerization process.

From Table 4, it can be observed that Si/Al ratio for FA1 and FA2 are 1.64 and 1.96, respectively. In contrast, the Si/Al ratio for FABS1 and FABS2 sands increased to 2.12 and 2.41. This is due to the pelletization process, where AAS (NaOH and Na_2SiO_3) is added to fly ash in order to produce the FAB sand. For the GPM cubes made with river, FABS1 and FABS2 sands, the Si/Al ratio is calculated as 2.91, 2.58, and 2.46, respectively. The greater compressive strength of GPM cubes made with river sand when compared with cubes made with FABS1 and FABS2, can be linked to the higher Si/Al ratio. As such, higher Si/Al ratio can enhance the degree of geopolymerization, leading to a more cross-linked and compact aluminosilicate network. This results in reduced porosity and improved structural integrity, thereby further increment in the compressive strength. The formation of longer —Si—O—Si— chains at higher Si levels can also contribute to a denser gel structure and enhanced strength (Davidovits 1991; Duxson et al. 2007). Understandably, these statements highlight the importance of optimizing Si/Al ratio for a better mechanical performance of GPM. These findings align with literature studies, which suggest that compressive strength in mortar samples improves with an increase in Si/Al ratio, up to a threshold of 3 (Pavithra et al. 2016b). Reddy et al. (2016) have recommended that SiO_2 and Al_2O_3 are the two major oxides that govern the geopolymeric network formation and in turn, the ultimate compressive strength of GPC. These observations imply that careful control and optimization of Si/Al ratio, particularly through raw material selection and mix design, play a pivotal role in tailoring the microstructure and enhancing the mechanical performance of GPM (Ray et al. 2025). By targeting Si/Al ratio close to the ideal threshold of 3, it is possible to develop more structurally efficient GPMs, thus contributing to high-performance construction materials.

Figs. 14–16 disclose the mineralogical compositions of FAs, FAB sands, river sand, and GPMs. In general, sharp peaks in XRD patterns signify crystalline structures while broad halos point to amorphous content of the material matrix (Chancey et al. 2010; Duxson et al. 2007). As seen in Fig. 14, natural river sand consists of quartz as a major crystalline phase. The presence of these crystalline silicate phases is beneficial, as they generate calcium-silicate-hydrate (CSH) gels in mortar and concrete samples (Muttashar et al. 2018). Principal crystalline minerals in FA1 and FA2 are identified as quartz (SiO_2) and mullite ($3Al_2O_3 \cdot 2SiO_2$) (Alterary and Marei 2021).

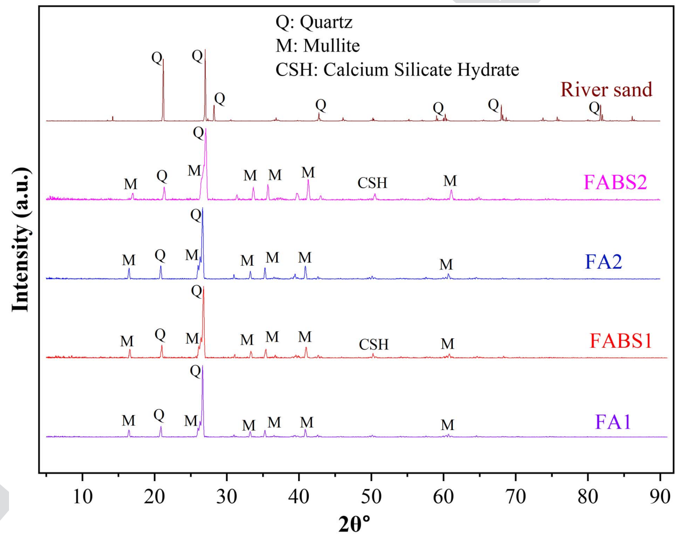

Fig. 14. X-ray diffractograms of FA1, FA2, FABS1, FABS2, and River sand.

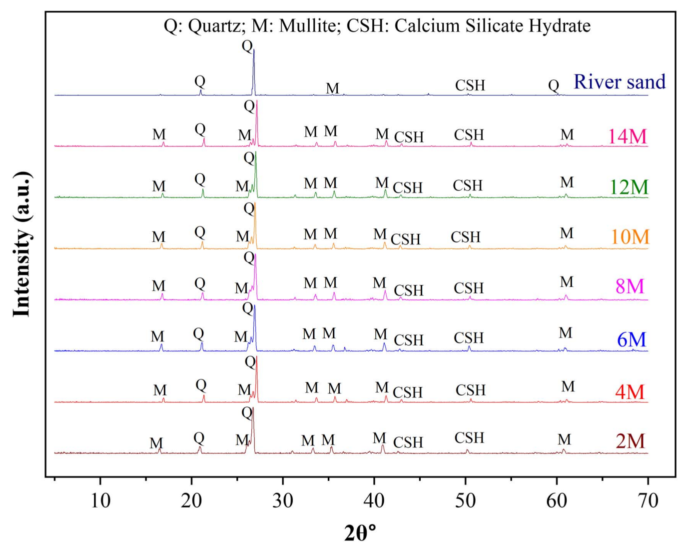

Fig. 15. X-ray diffractograms of GPM cubes made with FABS1.

Fig. 15 presents the diffractograms of GPM made with 100% river sand and 100% FABS1 (by altering NaOH molarity). It can be seen that GPM cubes made with 100% river sand show the reflections for quartz, mullite, and CSH gels. The minerals are basic constituents of river sand and FA2 while gels reflect that of successful geopolymerization. Evidently, mineral peaks in GPM with 100% FAB sand (Figs. 15 and 16) are found identical with those of FAB sand alone reflections (Fig. 14). It is prudent to interpret that the new reflections pertaining to CSH gels at 2θ (degrees) of 42.91 and 51.02

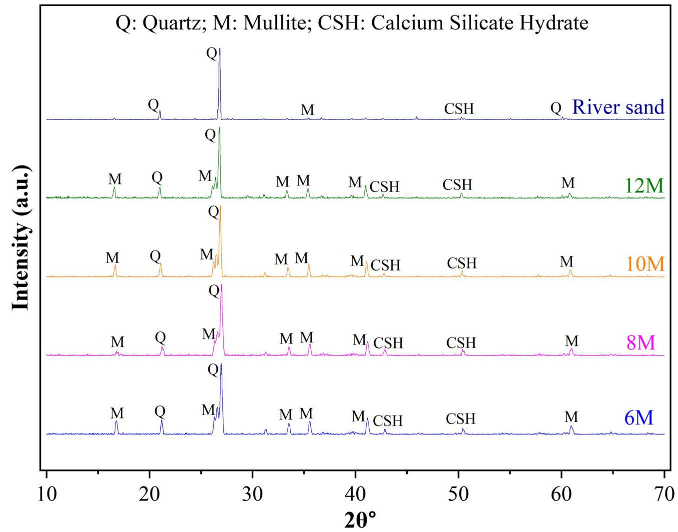

Fig. 16. X-ray diffractograms of GPM cubes made with FABS2.

in all the GPM made with FAB sands could have contributed to the higher compressive strength. Incidentally, the formation of CSH gel phases in fly ash (class F) based geopolymer fine aggregates are also reported in the literature by Parvathy et al. (2019) Sekhar and Rao (2024a, b). The earlier studies have reported that the formation of CSH gels within a geopolymeric matrix acts as micro-aggregates, which by enhancing the homogeneity and density of the binder, resulting in improved mechanical strength (Yip et al. 2005). Thus, it can be inferred from the significantly high compressive strength results (Figs. 8 and 9) that there are affluent formations of CSH gels in the GPM cubes made with FAB sand. Generally, the glassy phase of FA dissolves in an alkaline environment, releasing Si and Al ions. These ions subsequently undergo polymerization, forming aluminosilicate networks that help in solidifying the binder and thereby, inducing the desirable mechanical strength to the geopolymeric material (Pavithra et al. 2016a).

Leaching Results

The concentration of PTEs measured in leachates derived from GPMs made with FAB sands and exhibited highest compressive strength (Figs. 8 and 9) are shown in Table 5. For a better understanding of the effect of geopolymerization on heavy metal immobilization, PTEs measured for FA1, FA2, FABS1, and FABS2 are also presented in Table 5. The limiting values prescribed by international standards are also listed. Demonstrably, the measured concentrations of PTE are well below the limits set, highlighting that GPM from FAB sands do not pose any potential environmental hazard. These findings further indicate that FAB sand can widely be utilized as a resource material in construction applications. Concentrations of Fe, Na, Mg, K, and Ca (mg/l), are measured as 4.136, 67.104, 2.795, 20.813, and 12.014 in GPM made with FABS1, and 6.727, 66.597, 2.953, 24.525, and 12.72 in GPM made with FABS2.

Practical Applications in Construction Industry

In the pursuit of ecofriendly and durable construction materials, FAB sand, which aided in making GPM cubes with considerable high compressive strength, could become an emerging innovative construction material. The versatility of FAB sand could offer distinct advantages, as mentioned in Section 3.1, over the traditional options (Ng et al. 2018). Utilization of developed FAB sand as a replacement for river sand can mitigate environmental degradation caused by excessive sand mining.

According to ASTM C270 (ASTM 2024), the minimum compressive strength of Type M mortar, comprising cement-lime, mortar cement, or masonry cement mortar, is limited to 17.2 MPa at 28 days. In general, Type M mortar is known for its superior strength compared to other types, such as Type S, N, and O (ASTM C270-24 (ASTM 2024). Developed GPMs in the present study quietly exceed the benchmark strength set for Type M mortar. The strengths measured are in the range of 2945-MPa (Fig. 8) in the case of FABS1 GPM and 28–37 MPa (Fig. 9) in the case of FABS2 GPM. These impressive results establish that GPM made with FAB sand is ideal for manufacturing concrete blocks, bricks, and pavers, all of which are key to sustainable production of masonry materials, and to be used in infrastructure projects including construction of roads, highways and pavements where durability and strength are paramount (Cong and Cheng 2021). The density measurements of GPM cubes illustrate that FAB sand is an ideal material for lightweight construction, significantly curtailing dead loads while increasing design flexibility. This makes it highly suitable for both structural and nonstructural applications requiring weight reduction (Kumar et al. 2023).

Embodied Carbon Analysis and Sustainability Implications

To substantiate the sustainability claims, a quantitative comparison of embodied carbon is measured for traditional cement-based mortar and GPM incorporating river and FAB sand, as presented in Table 6. As per the literature, the embodied carbon value (kg CO_2-eq/kg) for raw materials such as cement, fly ash, river sand, water, 10 M NaOH solution, and Na_2SiO_3 solution is taken as 0.95, 0.01, 0.009, 0.0004, 0.8, and 0.4 (Adesina 2020; Mocharla et al. 2022; Myint and Shafique 2024). For the FAB sand, the embodied carbon is estimated as 0.05 kg CO_2-eq/kg, which is higher than river sand (0.009). Material quantities to produce 1 m^3 of cement mortar designed to achieve a compressive strength of 45 MPa are adapted (Ban and Ramli 2010). The total embodied

Table 5. Measured concentrations of potentially toxic elements in the leachates derived from FA1, FA2, FABS1, FABS2 and GPM made with FAB sands

Element	FA1 (mg/l)	FA2 (mg/l)	FABS1 (mg/l)	FABS2 (mg/l)	GPM with FABS1 (mg/l)	GPM with FABS2 (mg/l)	Permissible limits (mg/l) MoEF&CC (2016)	Permissible limits (mg/l) USEPA (2004)
As	0.078	0.120	0.064	0.093	0.059	0.082	5	5
Cd	0.002	0.001	0.001	0.029	0.004	0.006	1	1
Cr	0.099	0.026	0.028	0.015	0.012	0.006	5	5
Cu	0.016	0.016	0.010	0.004	0.006	0.012	25	100
Pb	0.089	0.005	0.035	0.003	0.002	0.002	5	5
Hg	0.003	0.006	0.002	0.002	0.013	0.002	0.2	0.2
Mn	0.010	0.065	0.069	0.047	0.055	0.089	10	—
Ni	0.049	0.016	0.011	0.013	0.025	0.051	20	7
Zn	0.090	0.036	0.030	0.015	0.161	0.244	250	500

Table 6. Embodied carbon calculations for cement based mortar (traditional mortar) and GPM made with river and FAB sands

Material	Cement based mortar		GPM with river sand		GPM with FAB sand	
	Quantity (kg/m^3)	Embodied carbon ($kg\ CO_2$-eq/m^3)	Quantity (kg/m^3)	Embodied carbon ($kg\ CO_2$-eq/m^3)	Quantity (kg/m^3)	Embodied carbon ($kg\ CO_2$-eq/m^3)
Cement	690	655.50	—	—	—	—
Water	262	0.11	—	—	—	—
River sand	1380	12.42	1239.17	11.15	—	—
Fly ash	—	—	760.83	7.61	905.96	9.05
FAB sand	—	—	—	—	1094.04	54.70
10 M NaOH solution	—	—	151.17	120.94	181.19	144.95
Na_2SiO_3 solution	—	—	228.25	91.30	271.79	108.71
Total Embodied carbon ($kg\ CO_2$-eq/m^3)	668		231		317	

carbon ($kg\ CO_2$-eq/m^3) for cement mortar is estimated at 668 while the same for GPM when using river sand is 231, which is markedly low representing 65.4% reduction in carbon emissions. Upon replacing river sand with developed FAB sand, the embodied carbon slightly increases to 317, which is still 52.5% lesser vis-à-vis traditional mortar. These observations are consistent with the results of the literature pertinent to geopolymer materials (Li et al. 2021). Furthermore, the manufacturing of GPM with FAB sand can promote sustainable construction by significantly lowering carbon emissions and enhancing resource efficiency (Parathi et al. 2021).

This dual substitution, cement with fly ash and river sand with FAB sand, not only reduces carbon emissions but also addresses two critical environmental challenges: overextraction of natural sand and fly ash disposal. Diverting fly ash from ash ponds and silos into high-performance construction materials like FAB sand reduces the environmental burden of dumping and mitigating the land degradation. For example, replacing 1 metric ton of cement with fly ash avoids nearly 950 kg of CO_2 emissions while also repurposing a material that would otherwise contribute to soil and water contamination. These results underscore the potential of GPM, particularly those incorporating alternate fine aggregates such as FAB sand, to substantially reduce the environmental footprint of construction materials while promoting circular economy principles through the valorization of industrial by-products. Furthermore, these results directly contribute to the United Nations sustainable development goals (SDGs), particularly SDG 9 (Industry, Innovation, and Infrastructure), by proposing FAB sand as a viable and innovative alternative to natural river sand in the construction industry. The study also supports SDG 12 (responsible consumption and production) through fostering the reuse of industrial by-products/wastes such as fly ash. In line with the listed global objectives, our research contributes to resource conservation and sustainable development while offering an ecofriendly solution.

Conclusions

In the present study, the effectiveness of FAB sand, successfully developed as an alternate substitute for river sand, in manufacturing the geopolymer mortar is demonstrated. The mechanical and water absorption properties of GPM are assessed. A key innovation of this study is the development of GPM cubes eliminating the use of natural resources such as river sand and cement, positioning GPM cubes as a driving force in the shift toward greener building practices. Based on the analysis of results and their interpretations, the following conclusions have been drawn:

1. It is successfully demonstrated that FAB sand, resembling excellently that of river sand within the particle size range from 4.75 to 0.075 mm, can be developed using industrial by-product such as fly ash alone and it is simple to adopt for all practical purposes.
2. The extensive characterization results authenticate that FAB sand complies excellently with the requirements for the construction activity, much like the river sand.
3. GPM cubes made with FABS1 have attained a maximum compressive strength of 45.1 MPa while cubes with FABS2 have yielded a maximum strength of 37.2 MPa.
4. The results highlight that compressive strength of GPM cubes increased with a curing age (7–28 days) and temperature (60°C–80°C).
5. The maximum and minimum density (kg/m^3) of GPM made with FAB sands are measured as 1,753 and 1,632. As the density measured less than 2,000 kg/m^3, it can be asserted that FAB sand is an ideal material for lightweight construction applications.
6. It is noticed that decrement in water absorption, from 20% to 9%, with an increase in compressive strength, from 26 to 45 MPa, does not exhibit any detrimental impact on the material's structural integrity.
7. Leaching results endorse that GPM made with FAB sand does not pose any environmental threat.
8. The results of embodied carbon reveal that GPM incorporating river sand and FAB sand reduces embodied carbon by 65.4% and 52.5% respectively, as compared with the conventional cement based mortar. This highlights their strong potential as environmentally sustainable alternatives.

Data Availability Statement

No data, models, or code were generated or used during the study.

Acknowledgments

The research work has been carried out under the sponsorship grant vide Ref. No.: DST/INT/SLOVENIA/2022/19 (DST/ICD/Slovenia/P-18/2021), Department of Science and Technology, Government of India, under aegis of Indo-Slovenia bilateral research program. The authors acknowledge Slovenian Research and Innovation Agency (ARIS): Program Group P2-027 and Projects BI-IN/22-24-018 and J1-4413. All authors sincerely express their thanks to the Department of Science and Technology for generous support and encouragement, in addition to knowledge support for carrying out this important research work. The authors are grateful to Vedanta Limited in Lanjigarh and National Thermal Power Corporation Limited in Kaniha for supplying fly ash. The authors would like to thank Mr. Vaddi Vamsi Krishna, Mr. Hari Prakash Raju Omkaram, and Mr. Kishore Konathala, students in the civil engineering department of G. Pulla Reddy Engineering College (Autonomous), Kurnool, for their help in carrying out the experimental work.

Author Contributions

Kummari Sekhar: Data curation; Investigation; Methodology; Visualization; Visualization; Writing – original draft; Writing – review and editing. Vesna Zalar Serjun: Methodology; Writing – review and editing. Bendadi Hanumantha Rao: Conceptualization; Methodology; Supervision; Writing – review and editing.

References

Adesina, A. 2020. "Performance and sustainability overview of alkali-activated self-compacting concrete." *Waste Disposal Sustainable Energy* 2 (3): 165–175. https://doi.org/10.1007/s42768-020-00045-w.

Agrawal, U. S., S. P. Wanjari, and D. N. Naresh. 2019. "Impact of replacement of natural river sand with geopolymer fly ash sand on hardened properties of concrete." *Constr. Build. Mater.* 209 (Jun): 499–507. https://doi.org/10.1016/j.conbuildmat.2019.03.134.

Alterary, S. S., and N. H. Marei. 2021. "Fly ash properties, characterization, and applications: A review." *J. King Saud Univ. - Sci.* 33 (6): 101536. https://doi.org/10.1016/j.jksus.2021.101536.

Ambily, P. S., C. Umarani, K. Ravisankar, P. R. Prem, B. H. Bharatkumar, and N. R. Iyer. 2015. "Studies on ultra high performance concrete incorporating copper slag as fine aggregate." *Constr. Build. Mater.* 77 (Feb): 233–240. https://doi.org/10.1016/j.conbuildmat.2014.12.092.

Anudeep, P., M. A. K. Reddy, V. C. Khed, M. Adamu, M. Varalakshmi, Y. E. Ibrahim, and O. S. Ahmed. 2024. "Effect of superplasticizer in geopolymer and alkali-activated cement mortar/concrete: A review." *Rev. Adv. Mater. Sci.* 63 (1): 20230173. https://doi.org/10.1515/rams-2023-0173.

Arulkumar, V., T. Nguyen, N. Tran, J. Black, Z. Zhang, X. Liu, and T. Ngo. 2025. "Thermo-mechanical treatment for enhancing the properties of recycled concrete aggregate." *J. Adv. Concr. Technol.* 23 (3): 168–183. https://doi.org/10.3151/jact.23.168.

ASTM. 2015. *Standard test method for flow of hydraulic cement mortar.* ASTM C1437-15. West Conshohocken, PA: ASTM.

ASTM. 2017a. *Standard specification for lightweight aggregates for structural concrete*. ASTM C330/C330M-17a. West Conshohocken, PA: ASTM.

ASTM. 2017b. *Standard test method for bulk density ('unit weight') and voids in aggregate*. ASTM C29/29M-17a. West Conshohocken, PA: ASTM.

ASTM. 2017c. *Standard test methods for particle-size distribution (gradation) of soils using sieve analysis*. ASTM D6913/D6913M - 17. West Conshohocken, PA: ASTM.

ASTM. 2020. *Standard test method for compressive strength of hydraulic cement mortars (Using 2-in. or [50-mm] cube specimens)*. ASTM C109/C109-20a. West Conshohocken, PA: ASTM.

ASTM. 2022. *Standard test method for rate of water absorption of masonry mortars*. ASTM 1403-22a. West Conshohocken, PA: ASTM.

ASTM. 2023. *Standard test method for relative density (specific gravity) and absorption of fine aggregate*. ASTM C128-22. West Conshohocken, PA: ASTM.

ASTM. 2024. *Standard specification for mortar for unit masonry.* ASTM C270-24. West Conshohocken, PA: ASTM.

Ban, C. C., and M. Ramli. 2010. "Optimization of mix proportion of high performance mortar for structural applications Cheah Chee ban and Mahyuddin Ramli sustainable housing research unit, school of housing, building and planning." *Concrete* 3 (4): 643–649. https://doi.org/10.3844/ajeassp.2010.643.649.

Baykal, G., and A. G. Döven. 2000. "Utilization of fly ash by pelletization process; theory, application areas and research results." *Resour. Conserv. Recycl.* 30 (1): 59–77. https://doi.org/10.1016/S0921-3449(00)00042-2.

BIS (Bureau of Indian Standards). 1963. *Methods of test for aggregates for concrete, Part 4: Mechanical properties*. IS 2386 Part 4. New Delhi, India: BIS.

BIS (Bureau of Indian Standards). 1988. "*Methods of physical tests for hydraulic cement, Part 7: Determination of compressive strength of masonry cement [CED 2: Cement and concrete]*. IS 4031 Part 7. New Delhi, India: BIS.

BIS (Bureau of Indian Standards). 2006. *Methods of physical tests for hydraulic cement, Part 6: Determination of compressive strength of hydraulic cement (other than masonry cement) [CED 2: Cement and concrete]*. IS 4031 Part 6. New Delhi, India: BIS.

Boobalan, S. C., V. Gayathri, G. Shyamala, D. Maruthachalam, and S. Rani. 2020. "Performance of sustainable concrete with crushed rock fines: A review." *IOP Conf. Ser.: Mater. Sci. Eng.* 981 (3): 032065. https://doi.org/10.1088/1757-899X/981/3/032065.

Chancey, R. T., P. Stutzman, M. C. G. Juenger, and D. W. Fowler. 2010. "Comprehensive phase characterization of crystalline and amorphous phases of a Class F fly ash." *Cem. Concr. Res.* 40 (1): 146–156. https://doi.org/10.1016/j.cemconres.2009.08.029.

Cong, P., and Y. Cheng. 2021. "Advances in geopolymer materials: A comprehensive review." *J. Traffic Transp. Eng. (English Ed.)* 8 (3): 283–314. https://doi.org/10.1016/j.jtte.2021.03.004.

Dash, M. K., S. K. Patro, and A. K. Rath. 2016. "Sustainable use of industrial-waste as partial replacement of fine aggregate for preparation of concrete: A review." *Int. J. Sustainable Built Environ.* 5 (2): 484–516. https://doi.org/10.1016/j.ijsbe.2016.04.006.

Davidovits, J. 1991. "Geopolymers inorganic polymeric new materials." *J. Therm. Anal.* 37: 1633–1656. https://doi.org/10.1007/BF01912193.

Duxson, P., A. Fernández-Jiménez, J. L. Provis, G. C. Lukey, A. Palomo, and J. S. J. Van Deventer. 2007. "Geopolymer technology: The current state of the art." *J. Mater. Sci.* 42 (9): 2917–2933. https://doi.org/10.1007/s10853-006-0637-z.

Ganesh Prabhu, G., J. H. Hyun, and Y. Y. Kim. 2014. "Effects of foundry sand as a fine aggregate in concrete production." *Constr. Build. Mater.* 70 (Nov): 514–521. https://doi.org/10.1016/j.conbuildmat.2014.07.070.

Gnanadurai, L. T., N. T. Renganathan, and C. G. Selvaraj. 2021. "Synthesis and characterization of synthetic sand by geopolymerization of industrial wastes (fly ash and GGBS) replacing the natural river sand." *Environ. Sci. Pollut. Res.* 28 (40): 56294–56304. https://doi.org/10.1007/s11356-021-14223-8.

Guo, Y., J. Xie, W. Zheng, and J. Li. 2018. "Effects of steel slag as fine aggregate on static and impact behaviours of concrete." *Constr. Build. Mater.* 192 (Dec): 194–201. https://doi.org/10.1016/j.conbuildmat.2018.10.129.

Gupta, N., and R. Siddique. 2020. "Durability characteristics of self-compacting concrete made with copper slag." *Constr. Build. Mater.* 247 (Jun): 118580. https://doi.org/10.1016/j.conbuildmat.2020.118580.

Hosen, M. A., M. I. Shammas, S. K. Shill, M. Z. Jumaat, U. J. Alengaram, R. Ahmmad, F. Althoey, A. B. M. S. Islam, and Y. Lin. 2021. "Investigation of structural characteristics of palm oil clinker based high-strength lightweight concrete comprising steel fibers." *J. Mater. Res. Technol.* 15 (Nov): 6736–6746. https://doi.org/10.1016/j.jmrt.2021.11.105.

Issa Fares, A., K. Md Abu Sohel, K. Al-Jabri, and A. Al-Saidy. 2023. "Influence of ferrochrome slag as coarse and fine aggregates on thermal and strength properties of concrete at high temperatures." *Constr. Build. Mater.* 400 (Oct): 132807. https://doi.org/10.1016/j.conbuildmat.2023.132807.

Kumar, K. P. 2018. "Characteristics of cement mortar with M-sand as replacement of fine aggregates." *Mater. Today: Proc.* 5 (11): 25412–25419. https://doi.org/10.1016/j.matpr.2018.10.346.

Kumar, P., D. Pasla, and T. J. Saravanan. 2023. "Self-compacting lightweight aggregate concrete and its properties: A review." *Constr. Build. Mater.* 375 (Apr): 130861. https://doi.org/10.1016/j.conbuildmat.2023.130861.

Lee, W. K. W., and J. S. J. Van Deventer. 2002. "Structural reorganisation of class F fly ash in alkaline silicate solutions." *Colloids Surf., A* 211 (1): 49–66. https://doi.org/10.1016/S0927-7757(02)00237-6.

Li, H., P. Gao, F. Xu, T. Sun, Y. Zhou, J. Zhu, C. Peng, and J. Lin. 2021. "Effect of fine aggregate particle characteristics on mechanical properties of fly ash-based geopolymer mortar." *Minerals* 11 (8). https://doi.org/10.3390/min11080897.

Liu, J., R. Niu, J. Hu, Y. Ren, W. Zhang, G. Liu, Z. Li, F. Xing, and J. Ren. 2023. "The performance and microstructure of alkali-activated artificial aggregates prepared from municipal solid waste incineration bottom ash." *Constr. Build. Mater.* 403 (Nov): 133012. https://doi.org/10.1016/j.conbuildmat.2023.133012.

MEFCC (Ministry of Environment, Forest and Climate Change). 2019. *Hazardous waste (management, handling & transboundary movement) rules*. MEFCC.

Mocharla, I. R., R. Selvam, V. Govindaraj, and M. Muthu. 2022. "Performance and life-cycle assessment of high-volume fly ash concrete mixes containing steel slag sand." *Constr. Build. Mater.* 341 (Jul): 127814. https://doi.org/10.1016/j.conbuildmat.2022.127814.

Muttashar, H. L., N. Bin Ali, M. A. Mohd Ariffin, and M. W. Hussin. 2018. "Microstructures and physical properties of waste garnets as a promising construction materials." *Case Stud. Constr. Mater.* 8 (Jun): 87–96. https://doi.org/10.1016/j.cscm.2017.12.001.

Myint, N. N., and M. Shafique. 2024. "Embodied carbon emissions of buildings: Taking a step towards net zero buildings." *Case Stud. Constr. Mater.* 20 (Jul): e03024. https://doi.org/10.1016/j.cscm.2024.e03024.

Nath, P., and P. K. Sarker. 2015. "Use of OPC to improve setting and early strength properties of low calcium fly ash geopolymer concrete cured at room temperature." *Cem. Concr. Compos.*, 55(Jan): 205–214. https://doi.org/10.1016/j.cemconcomp.2014.08.008.

Ng, C., U. J. Alengaram, L. S. Wong, K. H. Mo, M. Z. Jumaat, and S. Ramesh. 2018. "A review on microstructural study and compressive strength of geopolymer mortar, paste and concrete." *Constr. Build. Mater.* 186 (Oct): 550–576. https://doi.org/10.1016/j.conbuildmat.2018.07.075.

Parathi, S., P. Nagarajan, and S. A. Pallikkara. 2021. "Ecofriendly geopolymer concrete: A comprehensive review." *Clean Technol. Environ. Policy* 23 (6): 1701–1713. https://doi.org/10.1007/s10098-021-02085-0.

Patra, R. K., and B. B. Mukharjee. 2017. "Influence of incorporation of granulated blast furnace slag as replacement of fine aggregate on properties of concrete." *J. Cleaner Prod.* 165 (Nov): 468–476. https://doi.org/10.1016/j.jclepro.2017.07.125.

Paul, E. 2022. "Influence of superplasticizer on workability and strength of ambient cured alkali activated mortar." *Cleaner Mater.* 6 (Dec): 100152. https://doi.org/10.1016/j.clema.2022.100152.

Pavithra, P., M. Srinivasula Reddy, P. Dinakar, B. Hanumantha Rao, B. K. Satpathy, and A. N. Mohanty. 2016a. "A mix design procedure for geopolymer concrete with fly ash." *J. Cleaner Prod.* 133 (May): 117–125. https://doi.org/10.1016/j.jclepro.2016.05.041.

Pavithra, P., M. Srinivasula Reddy, P. Dinakar, B. Hanumantha Rao, B. K. Satpathy, and A. N. Mohanty. 2016b. "Effect of the $Na_2SiO_3/NaOH$ Ratio and NaOH molarity on the synthesis of fly ash-based geopolymer mortar." In *Proc., Geo-Chicago 2016*, 336–344. https://doi.org/10.1061/9780784480151.034.

Pilegis, M., D. Gardner, and R. Lark. 2016. "An investigation into the use of manufactured sand as a 100% replacement for fine aggregate in concrete." *Materials* 9 (6): 440. https://doi.org/10.3390/ma9060440.

Pratap, B., S. Mondal, and B. H. Rao. 2024. "Mechanical and durability assessment of phosphogypsum-bauxite residue-fly ash-based alkali-activated concrete." *Constr. Build. Mater.* 411 (Jan): 134670. https://doi.org/10.1016/j.conbuildmat.2023.134670.

Rai, B., S. Kumar, and K. Satish. 2016. "Effect of quarry waste on self-compacting concrete containing binary cementitious blends of fly ash and cement." *Adv. Mater. Sci. Eng.* 2016 (1): 1326960. https://doi.org/10.1155/2016/1326960.

Ray, V., K. Sekhar, N. G. Reddy, and B. H. Rao. 2025. "Beneficial utilization of waste heat for developing fly ash based geopolymer mortar." *Discover Civ. Eng.* 2 (1): 104. https://doi.org/10.1007/s44290-025-00262-4.

Reddy, M. S., P. Dinakar, and B. H. Rao. 2016. "A review of the influence of source material's oxide composition on the compressive strength of geopolymer concrete." *Microporous Mesoporous Mater.* 234 (Nov): 12–23. https://doi.org/10.1016/j.micromeso.2016.07.005.

Reddy, M. S., P. Dinakar, and B. H. Rao. 2018. "Mix design development of fly ash and ground granulated blast furnace slag based geopolymer concrete." *J. Build. Eng.* 20 (Nov): 712–722. https://doi.org/10.1016/j.jobe.2018.09.010.

Rentier, E. S., and L. H. Cammeraat. 2022. "The environmental impacts of river sand mining." *Sci. Total Environ.* 838 (May): 155877. https://doi.org/10.1016/j.scitotenv.2022.155877.

Romero, M., I. Padilla, J. L. García Calvo, P. Carballosa, F. Pedrosa, and A. López-Delgado. 2023. "Development of lightweight mortars using sustainable low-density glass aggregates from secondary raw materials." *Materials* 16 (18): 6281. https://doi.org/10.3390/ma16186281.

Sekhar, K., and B. H. Rao. 2024a. "Performance of geopolymeric process for developing fly ash based sand and its validation for engineering applications." *Innovative Infrastruct. Solutions* 9 (8): 313. https://doi.org/10.1007/s41062-024-01621-3.

Sekhar, K., and B. H. Rao. 2024b. "Assessment of fly ash based sand as a perspective alternate backfill material for stowing in mining activity." *Discover Geosci.* 2 (1): 79. https://doi.org/10.1007/s44288-024-00085-3.

Sekhar, K., and B. H. Rao. 2025. "Influence of gradation characteristics of precursor materials on the development of fly ash-based sand." In *Emerging trends in sustainable geotechnics*, edited by E. Koda, M. D. Vaverková, K. R. Reddy, and A. K. Agnihotri, 109–119. Singapore: Springer.

Sharma, A. K., and K. B. Anand. 2019. "Comparative study on synthesis and properties of geopolymer fine aggregate from fly ashes." *Constr. Build. Mater.* 198 (Feb): 359–367. https://doi.org/10.1016/J.CONBUILDMAT.2018.11.231.

Siddique, R. 2003. "Effect of fine aggregate replacement with Class F fly ash on the mechanical properties of concrete." *Cem. Concr. Res.* 33 (4): 539–547. https://doi.org/10.1016/S0008-8846(02)01000-1.

Singh, M., and R. Siddique. 2015. "Properties of concrete containing high volumes of coal bottom ash as fine aggregate." *J. Cleaner Prod.* 91 (Mar): 269–278. https://doi.org/10.1016/j.jclepro.2014.12.026.

Srivastava, A., and S. K. Singh. 2020. "Utilization of alternative sand for preparation of sustainable mortar: A review." *J. Cleaner Prod.* 253 (Apr): 119706. https://doi.org/10.1016/j.jclepro.2019.119706.

Sudam, P. A., M. Heeralal, and K. Srinivas. 2023. "Strength characteristics of geopolymer synthetic sand using fly ash." *J. Mater. Civ. Eng.* 35 (6): 04023119. https://doi.org/10.1061/JMCEE7.MTENG-14200.

Tran, N. P., T. Wang, T. N. Nguyen, H. Jin, and T. D. Ngo. 2024. "High-volume recycled glass cementitious and geopolymer composites incorporating graphene oxide." *Constr. Build. Mater.* 450 (Nov): 138476. https://doi.org/10.1016/j.conbuildmat.2024.138476.

USEPA. 1992. *Toxicity characteristic leaching procedure*. Washington, DC: USEPA.

USEPA. 2004. *Characteristics—Introduction and regulatory definitions*. Hazardous Waste Test Methods/SW-846. Washington, DC: USEPA.

Vu Hong Son, P., N. Van Nam, N. P. Tran, L. Le-Hoai, and T. D. Ngo. 2024. "Steel slag aggregate low-cement concrete: Engineering performance, microstructure and sustainability." *Constr. Build. Mater.* 436 (Jul): 136827. https://doi.org/10.1016/j.conbuildmat.2024.136827.

Xiao, J., C. Wang, T. Ding, and A. Akbarnezhad. 2018. "A recycled aggregate concrete high-rise building: Structural performance and embodied carbon footprint." *J. Cleaner Prod.* 199 (Oct): 868–881. https://doi.org/10.1016/j.jclepro.2018.07.210.

Yip, C. K., G. C. Lukey, and J. S. J. Van Deventer. 2005. "The coexistence of geopolymeric gel and calcium silicate hydrate at the early stage of alkaline activation." *Cem. Concr. Res.* 35 (9): 1688–1697. https://doi.org/10.1016/j.cemconres.2004.10.042.

Zailani, W. W. A., N. M. Apandi, A. Adesina, U. J. Alengaram, M. A. Faris, and M. F. M. Tahir. 2024. "Physico-mechanical properties of geopolymer mortars for repair applications: Impact of binder to sand ratio." *Constr. Build. Mater.* 412 (Nov): 134721. https://doi.org/10.1016/j.conbuildmat.2023.134721.

Queries

1. Please provide the ASCE Membership Grades for the authors who are members.
2. Please provide postal code for the author "Vesna Zalar Serjun" in affiliation footnotes.
3. Please check copyediting changes carefully throughout the article to ensure no changes have been made to your meaning.
4. Please check the hierarchy of section heading levels.
5. The text "STop of Form" has been deleted.
6. Please check all figures, figure citations, and figure captions to ensure they match and are in the correct order.
7. Please change section number to section heading per journal style.
8. The citation Parvathy et al. (2019) mentioned in this sentence is not present in the References list. Please provide the full details and we will insert it in the References list and link it to this citation.
9. Please note that section numbers are not permitted per journal style. Please change section numbers to section headings throughout.
10. This reference ASTM (2017b) is not mentioned anywhere in the text. ASCE style requires that entries in the References list must be cited at least once within the paper. Please indicate a place in the text, tables, or figures where we may insert a citation or indicate if the entry should be deleted from the References list.
11. Please provide page range for Li et al. (2021).
12. Please provide page range for MEFCC (2019).
13. Please provide the publisher or sponsor name and location (not the conference location) for Pavithra et al. (2016b).
14. This reference Sharma and Anand (2019) is not mentioned anywhere in the text. ASCE style requires that entries in the References list must be cited at least once within the paper. Please indicate a place in the text, tables, or figures where we may insert a citation or indicate if the entry should be deleted from the References list.